Chemically Engineered Nanoparticle-Protein Interface for Real Time Cellular Oxidative Stress Monitoring

Ying Jiang,
Department of Chemistry, University of Massachusetts Amherst, 710 North Pleasant Street, Amherst, MA 01003, USA

Dr. Ming Wang,
Department of Biomedical Engineering, Tufts University, 4 Colby Street, Medford, Massachusetts, 02115, USA

Joseph Hardie,
Department of Chemistry, University of Massachusetts Amherst, 710 North Pleasant Street, Amherst, MA 01003, USA

Gulen Yesilbag Tonga,
Department of Chemistry, University of Massachusetts Amherst, 710 North Pleasant Street, Amherst, MA 01003, USA

Moumita Ray,
Department of Chemistry, University of Massachusetts Amherst, 710 North Pleasant Street, Amherst, MA 01003, USA

Qiaobing Xu [Prof.], and
Department of Biomedical Engineering, Tufts University, 4 Colby Street, Medford, Massachusetts, 02115, USA

**Vincent M. Rotello**[*] **[Prof.]**
Department of Chemistry, University of Massachusetts Amherst, 710 North Pleasant Street, Amherst, MA 01003, USA

Graphical Abstract

Tel: (+1) 413-545-2058, rotello@chem.umass.edu.

Supporting Information
Supporting Information is available from the Wiley Online Library or from the author.

Co-engineered protein-nanoparticle interface → H_2O_2-mediated dosimetric response
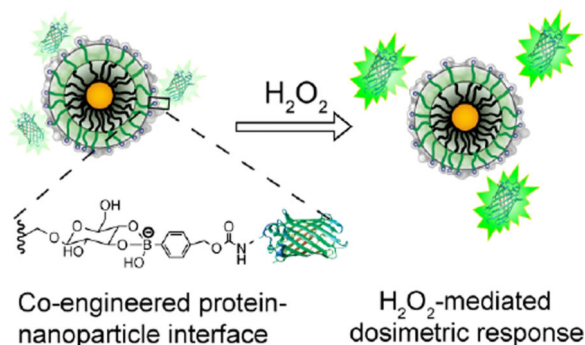
Keywords

cellular oxidative stress; gold nanoparticle; green fluorescent protein; chemically modified protein; hydrogen peroxide

Hydrogen peroxide is a product of cellular respiration and is one of the most important reactive oxygen species endogenously generated by cells.[1] H_2O_2 plays fundamental roles in multiple physiological and pathological processes, with the controlled generation of H_2O_2 essential to maintaining homeostasis and hence cell survival.[2] An overproduction of H_2O_2 results in oxidative stress that causes a range of diseases, including neurodegeneration,[3] diabetes,[4] and cancer.[5] The importance of H_2O_2 in biological processes necessitates the development of real-time sensing platforms for H_2O_2. Recently, fluorescent probes have been designed for H_2O_2 sensing, including small molecule fluorescent sensors,[6] synthetic cell-penetrating peptides,[7] genetically encoded fluorescent proteins,[8] and nanozymes.[9] However, the transient nature of ROS and the similarity of H_2O_2 with other ROS in terms of size and oxidative properties make peroxide sensing challenging.

Hybrid nanomaterials integrating synthetic nanomaterials with biomolecules including proteins and nucleic acids are important tools for chemical and biosensing.[10] These systems incorporate key elements of biomolecular function with the unique physical structural attributes of nanomaterials.[11] A substantial body of research exists on nucleic acid and peptide-functionalized nanomaterials, with protein-based systems rapidly emerging.[12] These systems generally use native proteins for sensing applications, providing recognition elements (e.g. antibodies) as well as enzymatic function. Genetic engineering of proteins provides a tool for creating NP-protein sensors with improved sensing selectivity and stability,[13] however the complicated genetic fusion process and limited functional group options for proteins provide limitations to this approach.

Chemical modification of proteins is an appealing alternative for endowing proteins with useful non-natural functionality and tunable properties.[14] We reasoned that integrating the strategies of chemically modified proteins with nanoparticle surface engineering would yield hybrid nanomaterials with synergetic functionality. We report here the creation of H_2O_2-responsive NP-protein conjugates and their ability to selectively monitor endogenous H_2O_2 production in live cells. In this study, we modify green fluorescent protein (GFP) with boronate functionality at the primary amine of lysine residues to provide a family of

phenylboronate-functionalized GFPs (PB-GFPs). These proteins react with galactose-functionalized gold nanoparticles (AuNP-Gal) via boronate ester formation (Figure 1). By tuning the extent of boronate modification of GFP through convenient chemical modifications, we demonstrate that the conjugation of PB-GFP with AuNP-Gal quenches the fluorescence of GFP depending on the number of boronate moieties conjugated to GFP. The PB-GFP/AuNP-Gal functionalization is peroxide-responsive: H_2O_2 catalyzes the bioorthogonal oxidation of boronate.[14, 1a] This oxidation disassembles the complex with concomitant restoration of GFP fluorescence (Figure 1), providing selective GFP-based on-off H_2O_2 detection for real time and *in situ* cellular oxidative stress monitoring.

Boronate-functionalized GFP was prepared through the reaction of GFP with 4-nitrophenyl 4-(4,5,5,5-tetramethyl-1,3,2-dioxaborolan-2-yl)benzyl carbonate (NBC) at different molar ratios (see experimental details in Supporting Information). The number of phenylboronic acid (PB) conjugated to GFP was determined using matrix-assisted laser desorption/ionization-time of flight (MALDI-TOF) mass spectroscopy (Figure S1, Supporting Information). In this study, GFP conjugated with 5, 9, and 20 PB per protein molecule, designated as PB5-GFP, PB9-GFP, and PB20-GFP, respectively, were complexed with gold nanoparticles (2 nm core) functionalized with galactose ligands (AuNP-Gal) that were prepared through the place-exchange reaction of 1-pentanethiol protected gold nanoparticles (AuNP-C5) and galactose ligands (Supporting Information).[15] The AuNPs were characterized using transmission electron microscopy (TEM) and dynamic light scattering (DLS) analysis (Figure S2, Supporting Information). In addition, GFP without PB conjugation (GFP) was used as a negative control to evaluate the effect of PB conjugation on enhancing protein-NP interaction.

The attachment between AuNP-Gal and PB-GFP was quantified by titrating GFP with AuNP and measuring the GFP fluorescence intensity change. The formation of a stable AuNP/PB-GFP interface efficiently quenches GFP fluorescence, providing straightforward observation of binding. As shown in Figure 2, the fluorescence of GFP solution (100 nM protein in PBS) shows little change with the addition of AuNP, indicating little binding between GFP and AuNP, in the presence of high concentration of salt (137 mM NaCl). In contrast, PB-GFP fluorescence was quenched with the addition of AuNP, depending on the number of PB units conjugated to GFP and the amount of AuNP added to PB-GFP. For example, PB20-GFP fluorescence was quenched up to 90% at an NP to protein ratio of 0.2, while 18% and 70% GFP emission quenching was observed for PB5-GFP and PB9-GFP respectively under the same conditions. This enhanced quenching indicates PB20-GFP protein has a stronger binding affinity with AuNP than that of PB5-GFP and PB9-GFP. The affinity and the Stern-Volmer constant of AuNP-Gal and PB20-GFP are substantially higher than PB5-GFP and PB9-GFP, as determined by the GFP fluorescence titration curve (Table S1 and Figure S3, Supporting Information)

We previously demonstrated that PB modified proteins are ROS-responsive, as hydrogen peroxide can cleave the boronate from the conjugated proteins through a bioorthogonal oxidization reaction.[14, 1a] We confirmed the ROS-responsive nature of PB-GFP by treating PB20-GFP protein with H_2O_2, and characterizing PB cleavage using MALDI-TOF. As shown in Figure S4 (Supporting Information), MALDI-TOF analysis indicated that the

treatment of PB20-GFP (30 μM protein) with 30 mM H_2O_2 resulted in a loss of fourteen PB groups from PB20-GFP. The disassembly of the AuNP/PB-GFP by H_2O_2 was then followed using fluorescence spectroscopy. As shown in Figure 3, the attachment of AuNP (25 nM) to PB20-GFP (100 nM protein in PBS) quenched GFP fluorescence by 90%. Treatment of the complex with 1 mM H_2O_2 for 30 min resulted in essentially complete restoration of GFP fluorescence. As shown in Figure S5 (Supporting Information), the fluorescence of AuNP/PB20-GFP complex (100 nM GFP and 25 nM AuNP-Gal) increased shortly after adding 1 mM H_2O_2, no further GFP fluorescence changed was observed after 25 minutes of incubation, indicating PB20-GFP protein was completely released from AuNP. The fast and dynamic process of the H_2O_2-regulated AuNP/PB20-GFP interface prompted us to study its potential application as an H_2O_2 assay.

Novel sensing platforms that discriminate different types of ROS and are capable of real time monitoring of ROS generation are important to study the physiological role of ROS and develop new disease diagnostic tools.[17] We evaluated the capability of the AuNP/PB20-GFP complex for sensitive and selective sensing of H_2O_2. As shown in Figure 4A, treatment of AuNP/PB20-GFP complex (100 nM PB20-GFP and 25 nM AuNP-Gal mixed in PBS containing 10% fetal bovine serum) with 20 μM H_2O_2, restored GFP fluorescence gradually within 2 h of incubation. Fast restoration of GFP fluorescence was observed for AuNP/PB20-GFP complex treated with a higher concentration of H_2O_2. For example, 150 μM H_2O_2 restored GFP fluorescence to more than 90% after 40 minutes of incubation. The response of the AuNP/ PB20-GFP complex is very selective toward H_2O_2 (Figure 4B). The addition of a variety of biologically relevant ROS, including hypochlorite (ClO-), H_2O_2, tert-butyl hydroperoxide (TBHP), nitroxide radical (NO·), and H_2O_2 in the presence of catalase (which acts to degrade H_2O_2), generated no perceptible response from the complex.

We next explored the utility of AuNP/PB20-GFP complex for real time monitoring of cellular oxidative stress. We first verified the use of the AuNP/PB20-GFP interface for H_2O_2 sensing in cell culture medium. To this end, human T lymphocyte Jurkat cells were spiked with different concentrations of H_2O_2, followed by an incubation with AuNP/PB20-GFP complex (100 nM PB20-GFP and 25 nM AuNP-Gal) and PB20-GFP fluorescence measurement. As shown in Figure 5A, Jurkat cells alone had no effect on disassembling the AuNP/PB20-GFP complex during the 2h of incubation, indicating the high stability of AuNP/PB20-GFP interface in biological media. The addition of 2.5 μM H_2O_2 resulted in a noticeable increase in fluorescence within 2h, while the GFP fluorescence was 2.5 times higher for AuNP/PB20-GFP complex spiked with 40 μM H_2O_2 (Figure 5A). Additionally, the GFP fluorescence is linearly correlated to the concentration of H_2O_2 spiked to the cell culture medium in the range of 2.5 to 40 μM (Figure S6, Supporting Information).

We next studied the capability of the AuNP/PB20-GFP interface to monitor endogenous H_2O_2 generated by Jurkat cells in the presence of the ROS stimulator, phorbol 12-myristate-13-acetate (PMA).[7, 14] PMA treatment activates NAPDH oxidase and induces the generation of superoxide, which is converted to ROS species including H_2O_2.[7] As shown in Figure 5B, Jurkat cells pretreated with 0.5 μM PMA before AuNP/PB20-GFP complex (100 nM PB20-GFP and 25 nM AuNP-Gal) incubation resulted in a significant enhancement of GFP fluorescence, compared to the cells without PMA stimulation. In

addition, when 0.5 mg/mL catalase was simultaneously added to PMA-stimulated Jurkat cells, no GFP fluorescence enhancement was observed due to consumption of the generated peroxide. By calibrating the GFP fluorescence of PMA-stimulated Jurkat cells to that of the AuNP/PB20-GFP complex in the presence of exogenous H_2O_2 after 120 minutes incubation, we estimated that the PMA-stimulation generated H_2O_2 at a rate of 0.49 nmol/10^4 cells/h, consistent with previous reports.[7]

In summary, we have co-engineered an NP-protein complex to provide an ROS-responsive system for real time H_2O_2 sensing and monitoring of cellular oxidative stress. This complex was created and modulated by the complexation between galactose-decorated gold nanoparticles and boronate modified protein. The assembled AuNP/PB-GFP interface is highly stable under a physiological environment, with GFP fluorescence generated by H_2O_2, providing timely biological dose estimates. The responsiveness of this system demonstrates the utility of co-engineering for creating functional and responsive synthetic-biological hybrid nanomaterials, a strategy that can be applied to many biological and physiological challenges.

Supplementary Material

Refer to Web version on PubMed Central for supplementary material.

Acknowledgments

References

1. a) Lippert AR, Van de Bittner GC, Chang CJ. Acc. Chem. Res. 2011; 44:793. [PubMed: 21834525] b) Nathan C, Cunningham-Bussel A. Nat. Rev. Immunol. 2013; 13:349. [PubMed: 23618831] c) Finkel T. Curr. Opin. Cell Biol. 2003; 15:247. [PubMed: 12648682]

2. a) Rhee SG. Science. 2006; 312:1882. [PubMed: 16809515] b) Shim MS, Xia Y. Angew. Chem. Int. Ed. 2013; 52:6926.

3. a) Mattson MP. Nature. 2004; 430:631. [PubMed: 15295589] b) Lin MT, Beal MF. Nature. 2006; 443:787. [PubMed: 17051205]

4. a) Houstis N, Rosen ED, Lander ES. Nature. 2006; 440:944. [PubMed: 16612386] b) Pop-Busui R, Sima A, Stevens M. Metab. Res. Rev. 2006; 22:257.

5. a) Fruehauf JP, Meysken FL. Clin. Cancer Res. 2007; 448:789.b) Finkel T, Serrano M, Blasco MA. Nature. 2007; 448:767. [PubMed: 17700693] c) Ishikawa K, Takenaga K, Akimoto M, Koshikawa N, Yamaguchi A, Imanishi H, Nakada K, Honma Y, Hayashi J. Science. 2008; 320:661. [PubMed: 18388260]

6. a) Miller EW, Tulyathan O, Isacoff EY, Chang CJ. Nat. Chem. Biol. 2007; 3:263. [PubMed: 17401379] b) Dickinson BC, Huynh C, Chang CJ. J. Am. Chem. Soc. 2010; 132:5906. [PubMed: 20361787] c) Abo M, Urano Y, Hanaoka K, Terai T, Komatsu T, Nagano T. J. Am. Chem. Soc. 2011; 133:10629. [PubMed: 21692459] d) Zhang R, Zhao J, Han G, Liu Z, Liu C, Zhang C, Liu B, Jiang C, Liu R, Zhao T, Han M-Y, Zhang Z. J. Am. Chem. Soc. 2016; 138:3769. [PubMed: 26938117] e) Jiang C, Liu R, Han G, Zhang Z. Chem. Commun. 2013; 49:6647.f) Zhang W, Li P, Yang F, Hu X, Sun C, Zhang W, Chen D, Tang B. J. Am. Chem. Soc. 2013; 135:14956. [PubMed: 24059644]

7. Weinstain R, Savariar EN, Felsen CN, Tsien RY. J. Am. Chem. Soc. 2014; 136:874. [PubMed: 24377760]

8. a) Ermakova YG, Bilan DS, Matlashov ME, Mishina NM, Markvicheva KN, Subach OM, Subach FV, Bogeski I, Hoth M, Enikolopov G, Belousov VV. Nat. Commun. 2014; 5:5222. [PubMed: 25330925] b) Belousov VV, Fradkov AF, Lukyanov KA, Staroverov DB, Shakhbazov KS, Terskikh AV, Lukyanov S. Nat. Methods. 2006; 3:281. [PubMed: 16554833]

9. a) Liu B, Sun Z, Huang PJ, Liu J. J. Am. Chem. Soc. 2015; 137:1290–1295. [PubMed: 25574932] b) Ornatska M, Sharpe E, Andreescu D, Andreescu S. Anal. Chem. 2011; 83:4273. [PubMed: 21524141]

10. a) Jiang Y, Zhao H, Lin Y, Zhu N, Ma Y, Mao LQ. Angew. Chem. Int. Ed. 2010; 49:4800.b) Saha K, Agasti SS, Kim C, Li X, Rotello VM. Chem. Rev. 2012; 112:2739. [PubMed: 22295941] c) You CC, Miranda OR, Gider B, Ghosh PS, Kim IB, Erdogan B, Krovi SA, Bunz UHF, Rotello VM. Nat Nanotechnol. 2007; 2:318. [PubMed: 18654291] d) Cutler JI, Auyeung E, Mirkin CA. J. Am. Chem. Soc. 2012; 134:1376. [PubMed: 22229439]

11. Rana S, Yeh YC, Rotello VM. Curr. Opin. Chem. Biol. 2010; 14:828. [PubMed: 21035376]

12. Rana S, Le NDB, Mout R, Saha K, Tonga GY, Bain RES, Miranda OR, Rotello CM, Rotello VM. Nat. Nanotechnol. 2015; 10:65. [PubMed: 25502312]

13. Mout R, Tonga GY, Ray M, Moyano DF, Xing Y, Rotello VM. Nanoscale. 2014; 6:8873. [PubMed: 24960536]

14. Wang M, Sun S, Neufeld CI, Perez-Ramirez B, Xu Q. Angew. Chem. Int. Ed. 2014; 53:13444.

15. a) Elci SG, Moyano DF, Rana S, Tonga G, Philips R, Bunz U, Rotello VM. Chem. Sci. 2013; 4:2076.b) Brust M, Walker M, Bethell D, Schiffrin DJ, Whyman R. J. Chem. Soc. Chem. Commun. 1994:801.

16. You CC, De M, Han G, Rotello VM. J. Am. Chem. Soc. 2005; 127:12873. [PubMed: 16159281]

17. a) Broaders KE, Grandhe S, Frechet JMJ. J. Am. Chem. Soc. 2011; 133:756. [PubMed: 21171594] b) de Gracia Lux C, Joshi-Barr S, Nguyen T, Mahmoud E, Schopf E, Fomina N, Almutairi A. J. Am. Chem. Soc. 2012; 134:15758. [PubMed: 22946840]
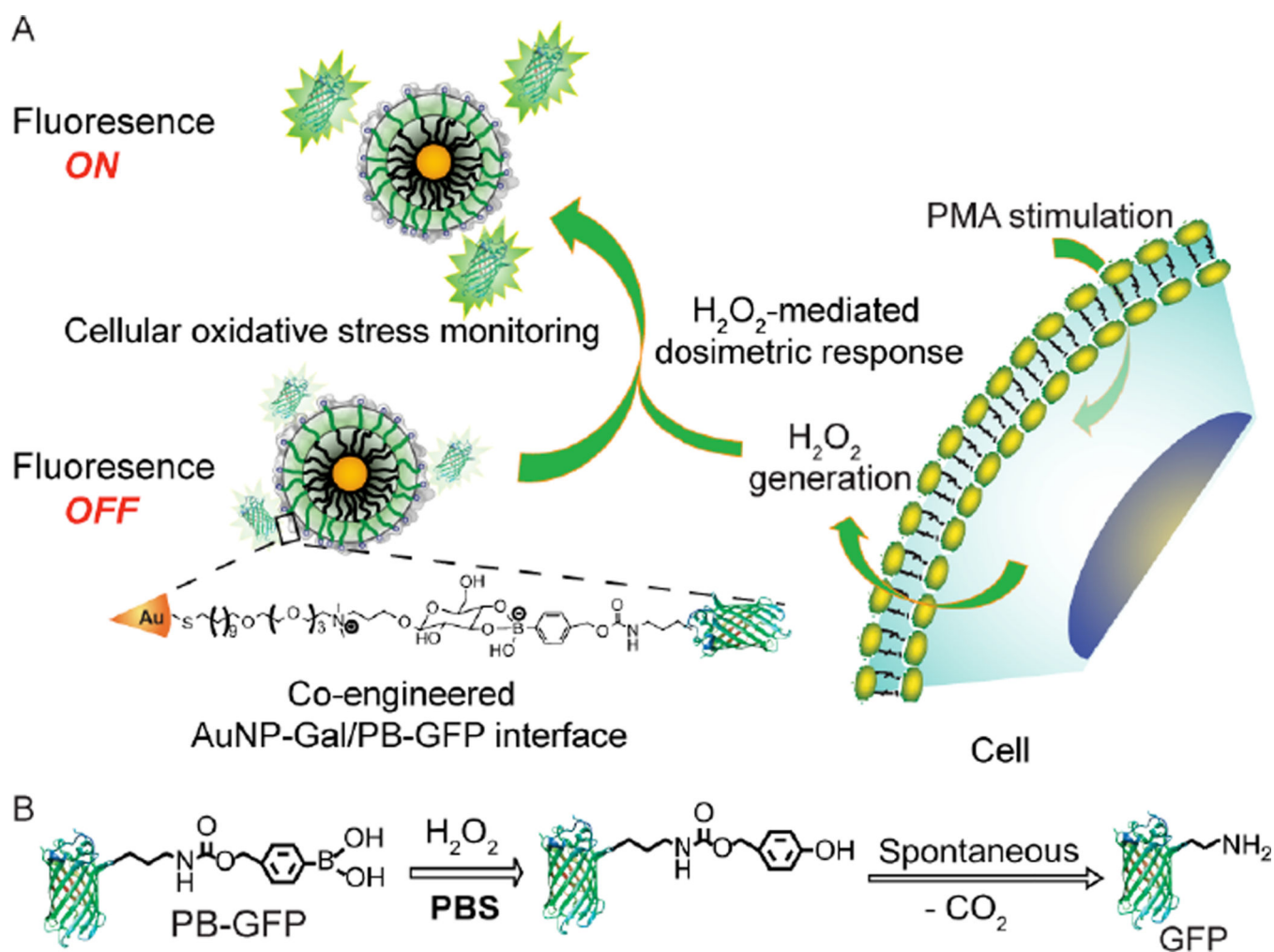
Figure 1.
Chemically engineered AuNP/PB-GFP interface for H_2O_2 sensing. A) Schematic illustrating the interfacing of AuNP-Gal with PB-GFP, and phorbol 12-myristate-13-acetate (PMA) stimulated *in situ* H_2O_2 generation modulated GFP release from the AuNP/PB-GFP interface. B) Reaction mechanism of PB-GFP with H_2O_2 catalyzed bioorthogonal PB cleavage.
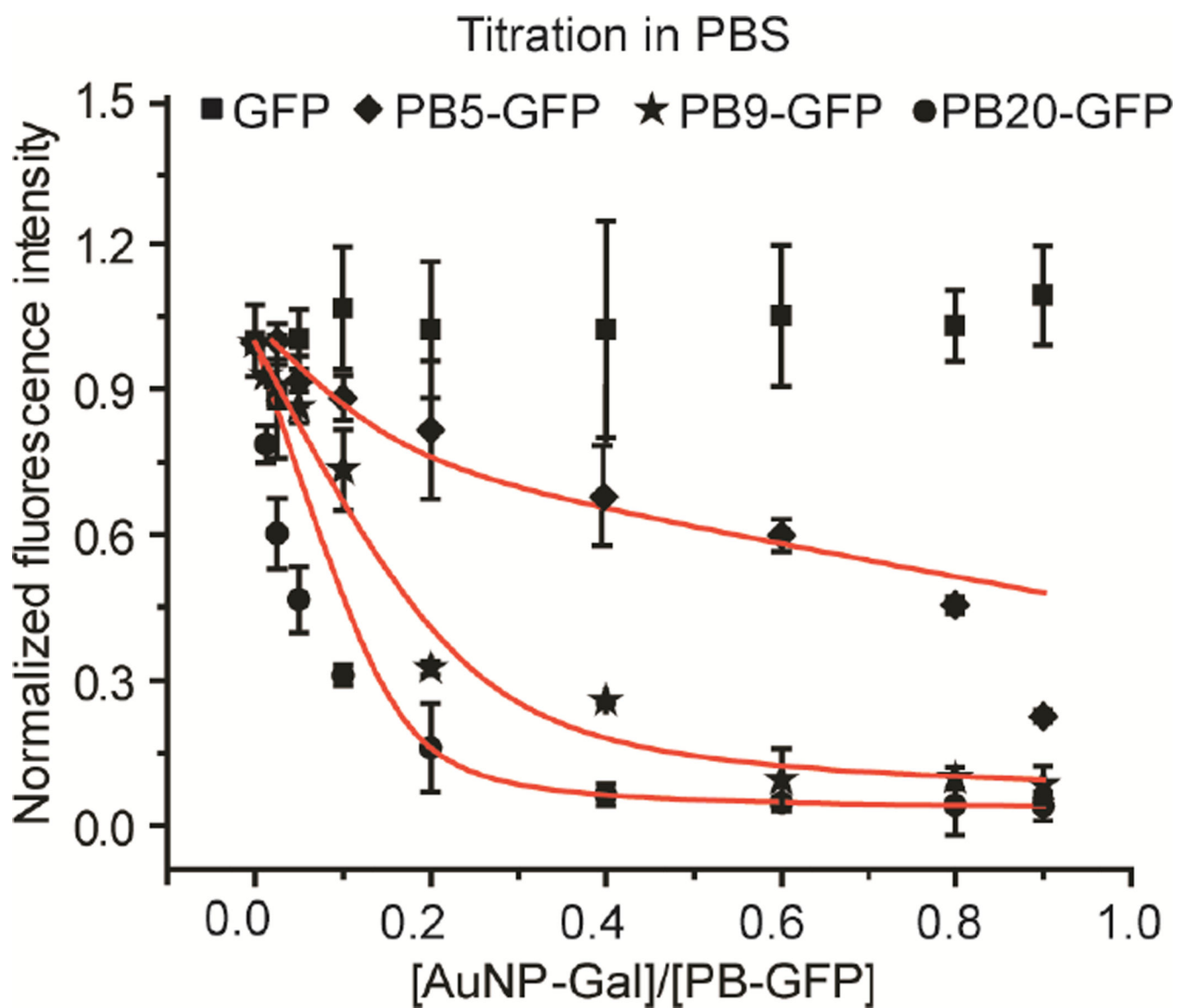
Figure 2.
Fluorescence titration of PB-GFP with AuNP-Gal. 100 nM protein was mixed with increased amounts of AuNP-Gal in PBS, and after incubation for 15 min, the fluorescence intensity of GFP was recorded. GFP fluorescence (λ_{ex} = 475 nm, λ_{em} = 510 nm) in the presence of AuNP-Gal was normalized to that without AuNP-Gal addition. Each titration experiment was performed in three replicates. The red solid lines represent the best curve fitting using the previously reported method.[16]
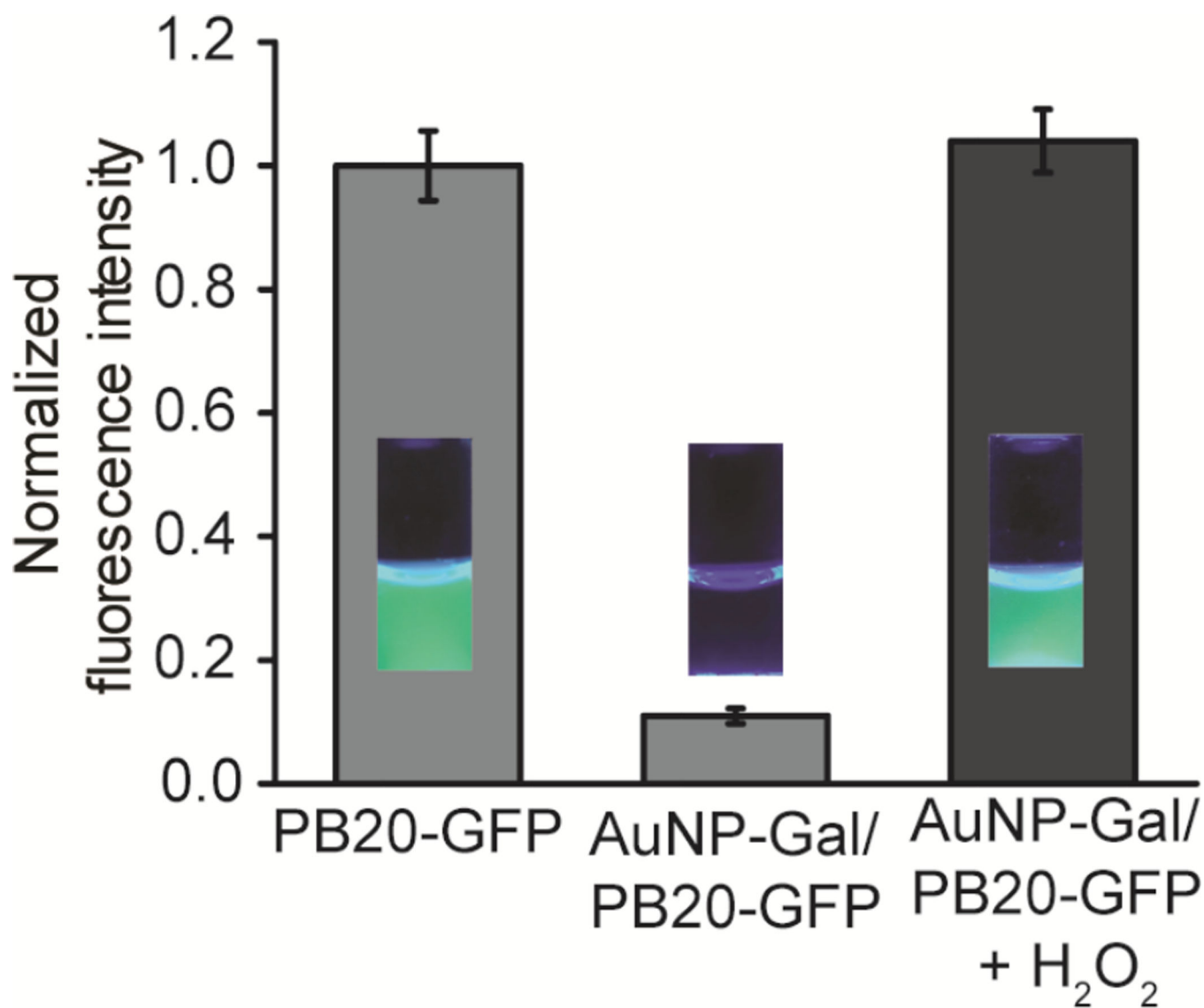
Figure 3.
Fluorescence intensity of PB20-GFP, and AuNP-Gal/PB20-GFP complexes before and after addition of H_2O_2. The AuNP-Gal/PB20-GFP conjugates were prepared by incubating PB20-GFP (100 nM) with a fixed PB20-GFP to AuNP-Gal ratio (4:1) for 15 min. All GFP fluorescence values were presented relative to the PB20-GFP control. Error bar represents the standard deviation of three independent studies. Photograph showing fluorescence of PB20-GFP, AuNP-Gal/PB20-GFP complexes, and AuNP-Gal/PB20-GFP complexes upon addition of H_2O_2 under ultraviolet light.
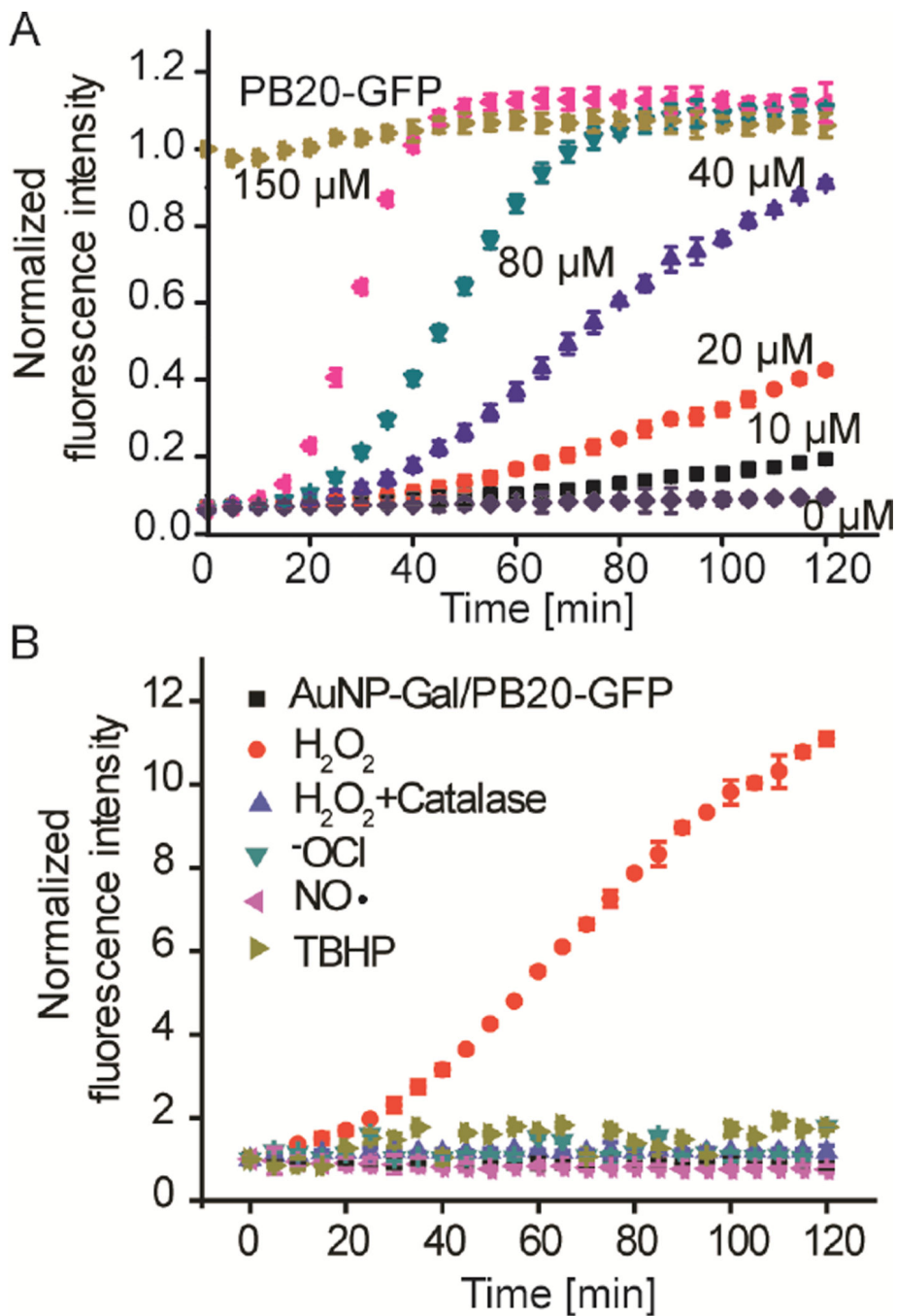
Figure 4.

H_2O_2 concentration-dependent and selective modulation of the AuNP-Gal/PB20-GFP interface. A) The fluorescence response of AuNP-Gal/PB20-GFP (100 nM PB20-GFP) upon the addition of increasing concentrations of H_2O_2 in PBS containing 10% FBS. The fluorescence response was presented relative to the PB20-GFP control. B) Time-dependent fluorescence response of AuNP-Gal/ PB20-GFP (100 nM PB20-GFP) upon addition of H_2O_2 (50 µM) or other ROS (100 µM) as indicated in PBS containing 10% FBS. Catalase (0.5 mg/mL) was added to verify the role of H_2O_2 in modulating AuNP/PB20-GFP

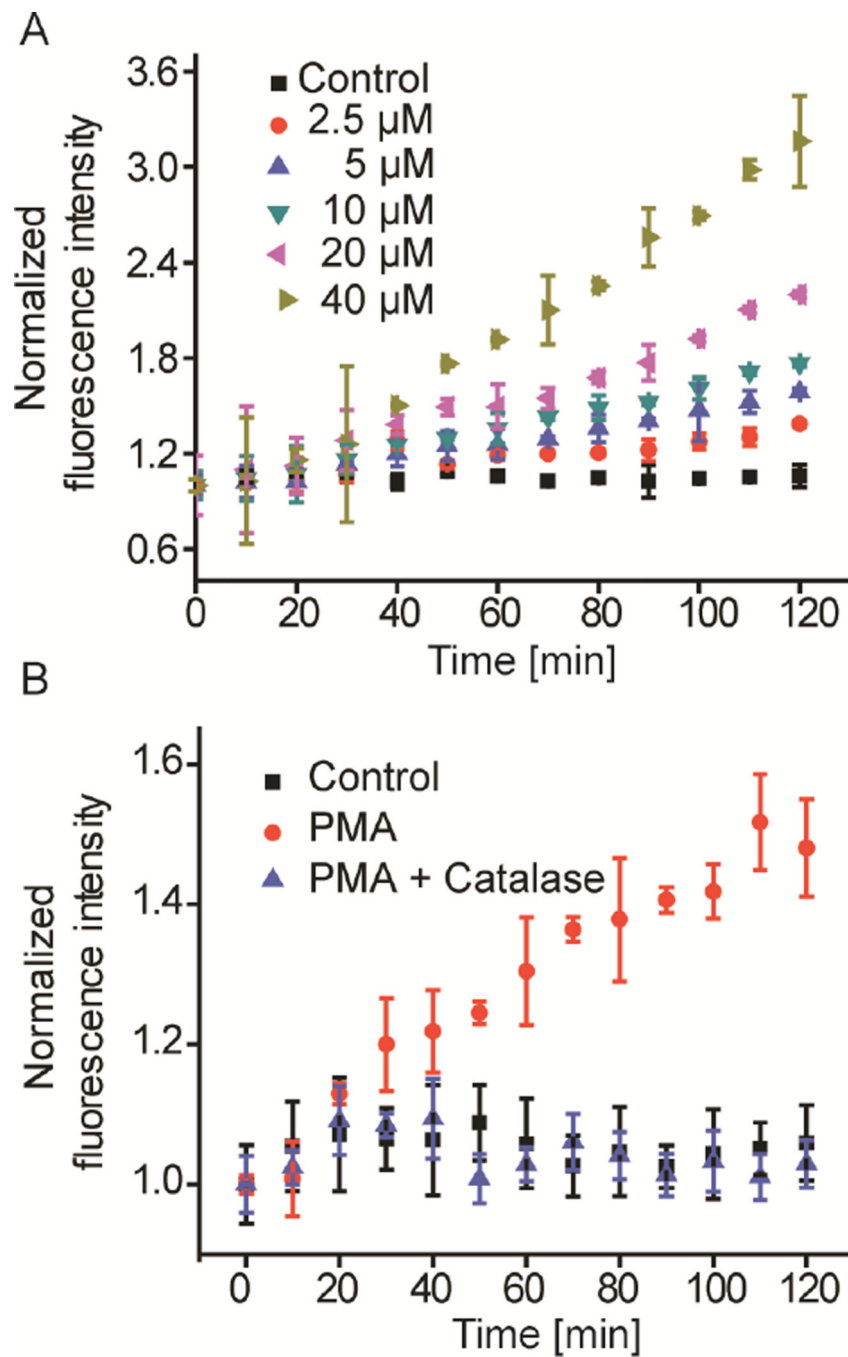interface. The fluorescence response was presented relative to the AuNP-Gal/ PB20-GFP controls.

Figure 5.

Detection of H_2O_2 using the AuNP-Gal/PB20-GFP in cellular environment. (a) Time-dependent fluorescence response of AuNP-Gal/PB20-GFP complex (100 nM of PB20-GFP) added to Jurkat cells spiked with different concentrations of H_2O_2. The fluorescence response was presented relative to the AuNP-Gal/PB20-GFP controls. (b) The fluorescence response of AuNP-Gal/PB20-GFP (100 nM of PB20-GFP) incubated with Jurkat cells stimulated with PMA (0.5 μM), or incubated with catalase (0.5 mg/mL) and PMA (0.5 μM)

simultaneously. All fluorescence values were presented relative to the AuNP-Gal/PB20-GFP controls. Error bar represents the standard deviation of three independent studies.